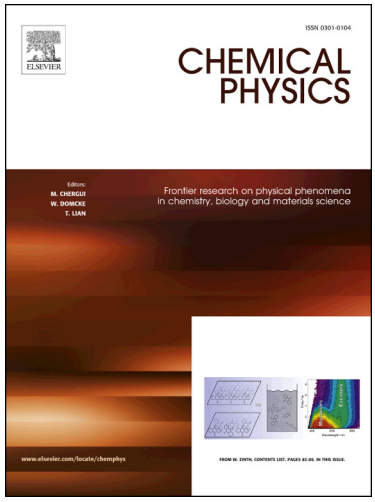

Calculation of intermolecular potentials for H_2–H_2 and H_2–O_2 dimers *ab initio* and prediction of second virial coefficients

Tat Pham Van, Ulrich K. Deiters

PII: S0301-0104(15)00169-X
DOI: http://dx.doi.org/10.1016/j.chemphys.2015.05.025
Reference: CHEMPH 9331

To appear in: *Chemical Physics*

Received Date: 5 April 2015
Accepted Date: 29 May 2015

Please cite this article as: T.P. Van, U.K. Deiters, Calculation of intermolecular potentials for H_2–H_2 and H_2–O_2 dimers *ab initio* and prediction of second virial coefficients, *Chemical Physics* (2015), doi: http://dx.doi.org/10.1016/j.chemphys.2015.05.025

Calculation of intermolecular potentials for H_2–H_2 and H_2–O_2 dimers *ab initio* and prediction of second virial coefficients

Tat Pham Van[1] and Ulrich K. Deiters[2]

[1]Faculty of Science and Technology, Hoa Sen University, Vietnam
[2]Institute of Physical Chemistry, University of Cologne,
Luxemburger Str. 116, D-50939 Köln, Germany

Abstract

The intermolecular interaction potentials of the dimers H_2–H_2 and H_2–O_2 were calculated from quan-tum mechanics, using coupled-cluster theory CCSD(T) and correlation-consistent basis sets aug-cc-pV*m*Z (*m* = 2, 3); the results were extrapolated to the basis set limit aug-cc-pV23Z. The interaction energies were corrected for the basis set superposition error with the counterpoise scheme. For comparison also Møller–Plesset perturbation theory (at levels 2 to 4) with the basis sets aug-cc-pVTZ were considered, but the results proved inferior. The quantum mechanical results were used to construct analytical pair potential functions. From these functions the second virial coefficients of hydrogen and the cross virial coefficients of the hydrogen–oxygen system were obtained by integration; in both cases corrections for quantum effects were included. The results agree well with experimental data, if available, or with empirical correlations.

1. Introduction

Computer simulations have become indispensable tools for studying fluids and fluid mixtures. They can generate structural, thermodynamic as well as transport properties consistently without the need to introduce artificial simplifications as required by, e.g., integral equation techniques, statistical ther-modynamic perturbation theory. Computer simulation techniques, Monte Carlo as well as Molecular Dynamics, cannot work without some input, however: It is necessary to know the interaction potentials of the systems under study.

The usual procedure is to assume a simple model potential, e.g., the Lennard-Jones pair potential, fit its parameters to suitable experimental data, and then to perform the simulation. Such a simulation is no longer predictive, because it requires experimental input of the same kind that is produces. This can sometimes be a severe limitation, namely if experimental data are scarce.

An example of such a system is the fluid mixture (H_2 + O_2). Its thermodynamic properties are important for the design of efficient rocket engines [1,2] and may have some bearing for future hydrogen storage and fuel cell technologies, but there are remarkably few publications of experimental results only— for evident reasons.

Recently an alternative approach has become feasible, for which the name “global simulation” has been coined [3]. It consists of a calculation of intermolecular potentials by quantum mechanical methods, followed by computer simulations and — eventually — calculations with equations of state fitted to the simulations results, in order to obtain properties that are not accessible to simulations.

Such global simulations have been reported for the noble gases, where it is now possible to predict the vapour–liquid phase equilibria without recourse to experimental data with an accuracy comparable to the experimental uncertainty. One of the first attempts that achieved near-experimental accuracy was that of Deiters, Hloucha and Leonhard [4] for neon. Further global simulation attempts for noble gases were published by the groups of Eggenberger and Huber [5–9], Sandler [10], and Malijevsky´ [11]. Using a functional form for the dispersion potentials of argon and krypton proposed by Korona et al. [12], Nasrabad and Deiters even predicted phase high-pressure vapour–liquid phase equilibria of noble-gas mixtures [13,14,15]. Other mixed-dimer pair potentials for noble gases were published by López Cacheiro et al. [16], but not used for phase equilibria predictions, yet.

The development of *ab initio* pair potentials for molecules is much more complicated because of the angular degrees of freedom of molecular motion, but for some simple molecules such potentials have al-ready been constructed: Leonhard and Deiters used a 5-site Morse potential to represent the pair potential of nitrogen [17] and were able to predict vapour pressures and orthobaric densities. Bock et al. also used a 5-site pair potential for carbon dioxide [18]; they furthermore applied the first-order quantum correc-tion to the 2nd virial coefficients developed by Pack [19]. Naicker et al. used SAPT (symmetry-adapted perturbation theory) to develop a 3-site pair potential for hydrogen chloride [20], based on Korona’s func-tion and a modified Morse potential; they then successfully predicted the vapour–liquid phase equilibria of hydrogen chloride with GEMC (Gibbs ensemble Monte Carlo [21]) simulations.

We note in passing that there is a wealth of *ab initio* pair potential work on water dating back even to 1973 [3]. In liquid water, however, the dominant intermolecular interactions are the hydrogen bond and electrostatic forces, the energy of which can be calculated with a decent accuracy even at SCF level, whereas the calculation of dispersion forces requires computationally expensive high-level

theories. Similarly, there are many publications using a hybrid approach, i.e., computing structures and charge distri-butions of molecules with advanced quantum mechanical methods, but using empirical functions for the dispersion contributions. With this approach it is possible to deal with relatively large molecules, but as it is not fully predictive, it is not within the scope of this work.

In this work we report quantum mechanical calculations at a sufficiently high level of approximation to obtain pair potential data of the H_2–H_2 and the H_2–O_2 dimers. These data are then represented by analytical pair potential functions. These in turn are used to calculate 2nd virial coefficients. This calculation involves exact expressions only and can be performed without any loss of accuracy. The 2nd virial coefficents can then be compared to experimental data — as far as such data are available. They can furthermore be used to determine the parameters of a suitable equation of state. From there it is in principle possible to predict for phase equilibria and excess volumes of (H_2 + O_2) mixtures.

There have been other attempts to develop a pair potential function for hydrogen. A potential was published by Diep and Johnson, who performed calculations with post-SCF methods MP2, MP3, MP4, and CCSD(T) and with the basis sets aug-cc-pV*m*Z (*m* = 2, 3), including extrapolation to the basis set limit [22,23]. This pair potential, however, uses a spherical harmonics expansion to account for the anisotropy of interaction. Such an approach can become problematic, however, if repulsion at short ranges becomes the dominant feature of a fluid, e.g., in a dense liquid state.

2. Computational details

2.1. Molecular orientation

In this work hydrogen and oxygen molecules are represented as 5-site models, with two sites placed on the atoms (H or O), one site in the center of gravity (M), and two sites halfways between the atoms and the center (N). The molecules are treated as rigid; the interatomic distances are set to 0.74130 Å for hydrogen and 1.20741 Å for oxygen [24].

As hydrogen and oygen are linear molecules, the intermolecular pair potential is a function of distance r (distance between the centers of gravitiy) and three angular coordinates, α, β, and ϕ, which are explained in Fig. 1.

Interaction energies were calculated for all values of r from 2.6 to 15 Å with increment 0.2 Å; the angles α, β, and ϕ were varied from 0 to 180° with increment 45°. Care was taken to recognize identical configurations in order to reduce the computational workload.

2.2. Quantum chemical calculations

The Hartree–Fock SCF method is a widely used method in quantum chemistry; it had proven useful for the calculation of chemical bond energies and even of hydrogen bonding energies. Dispersion forces, however, are caused by electron correlations, and these effects are excluded in SCF calculations.

A full configuration interaction treatment (CI) of electron correlations requires enormous computational resources and is at present usually not practical. Fortunately there are several other post-SCF methods that can capture at least a part of the electron correlation effects, e.g., Møller–Plesset perturbation theory (MP) and coupled-cluster methods (CC). Experience shows that especially the CCSD(T) method appears to account for the most significant electron correlation efects. It is therefore used in this work. But the results are compared with the perturbation theory at levels MP2, MP3, and MP4 will be discussed, too.

Because of the diffuse, wide-range nature of dispersion force fields it is necessary to adopt appropriate basis sets. Here we use the correlation-consistent basis sets of Dunning et al. [25]: aug-cc-pVDZ (for oxygen: 10s5p2d/4s3p2d, for hydrogen: 5s2p/3s2p) and aug-cc-pVTZ (for oxygen: 12s6p3d2f/5s4p3d2f, for hydrogen: 6s3p2d/4s3p2d). The *ab initio* energy results were corrected for the basis set superposition error (BSSE) with the counterpoise correction method proposed by Boys and Bernardi [26]:

$$\Delta E = E_{AB} - E_{Ab} - E_{aB} \tag{1}$$

where E_{AB} denotes the total electronic energy of a dimer AB, E_{Ab} the energy of a dimer consisting of an A atom and a B ghost atom (an atom without nucleus and electrons, but having its orbitals), and E_{aB} vice versa.

The electronic energies are then extrapolated to the basis set limit [27–30]:

$$\Delta E(m) = \Delta E(\infty) + cm^{-3} \tag{2}$$

with m = 2 (for the aug-cc-pVDZ basis set) or 3 (for aug-cc-pVTZ). If results for two basis sets are available, it is possible to calculate the energy value for an infinite basis set from Eq. (2); this result is referred to as aug-cc-pV23Z below.

Another method for obtaining basis sets with a sufficiently diffuse character is the inclusion of bond functions. It is our experience, however, that the extrapolation scheme is adequate [13,14,17,31].

All quantum chemical calculations were carried out with the Gaussian03™ program package [32]. The influence of the choice of the theory level is shown in Figs. 2 and 3 for a special molecular configuration, the T-configuration of Fig. 1.

Figs. 4 and 5 similarly demonstrate the influence of the basis set. It must be pointed out that the basis sets most commonly used for calculations of chemical bonds, turn out to be totally insufficient for the purpose of calculating intermolecular potentials.

The locations and depths of the potential minima for four different dimer configurations are given in Table 1. In all cases the extrapolation to the basis set limit has a significant effect on the calculated energies.

In order to verify that the calculation method and the basis set can yield an adequacy to describe for dimers hydrogen and oxygen, we performed calculations without restrictions of the intramolecular bond length for a T-configuration: The results, listed in Table 2, show that the CCSD(T) calculation with the extrapolated basis set gives results within 1% of the experimental values. This also proves that the molecules are not significantly deformed upon making contact with each other, or that vibrational excitation is not to be expected with low-speed collisions.

The potential energies of the dimers H_2–H_2 and H_2– O_2 for all distances and orientations, calculated with the CCSD(T) method and the aug-cc-pV*m*Z basis sets, are given in Table 7.

3. The pair potential function

For the calculation of virial coefficients, but especially for the use within computer simulations, it is desirable to represent the *ab initio* pair potential data by an analytic function. As the molecules considered here are not spherical, the construction of an accurate, yet not too computationally expensive function is not a trivial task.

Modelling the molecular anisotropy by spherical harmonics is possible in principle, but not attempted here for reasons explained in the Introduction. Instead, a multi-center potential is proposed. Previous work on nitrogen [17,33] and carbon dioxide [18] had shown that 2-site or even 3-site molecular models did not represent the *ab initio* data well, but that 5-site models were sufficient. In principle such a 5-site model leads to a pair potential consisting of 25 spherical site-site interactions, but because of molecular symmetry only six different site-site potentials have to be fitted for hydrogen, and 8 for the hydrogen–oxygen dimer.

For the construction of the pair potential function two different functional forms were explored. The first one had been used by Bock et al. for carbon dioxide [18]:

$$u = \sum_{i=1}^{5}\sum_{j=1}^{5}\left[D_e^{ij} e^{-\alpha_{ij} r_{ij}} + f_1(r_{ij}) \sum_{n=6,8,10} \frac{C_{ij,n}}{r_{ij}^n} + f_2(r_{ij}) \frac{q_i q_j}{4\pi\epsilon_0 r_{ij}} \right] \tag{3}$$

with $f_1(r_{ij}) = (1 + e^{-2(\delta_{ij} r_{ij} - 2)})^{-15}$ and $f_2(r_{ij}) = 1 - e^{-\zeta_{ij} r_{ij}}$

The other functional form was proposed by Naicker et al. [20], originally used for hydrogen chloride

$$u = \sum_{i=1}^{5}\sum_{j=1}^{5}\left[D_e^{ij} e^{-\alpha_{ij} r_{ij}} + f_1(r_{ij}) \sum_{n=6,8,10,12} \frac{C_{ij,n}}{r_{ij}^n} + f_2(r_{ij}) \frac{q_i q_j}{4\pi\epsilon_0 r_{ij}} \right] \tag{4}$$

with $f_1(r_{ij}) = 1 - e^{-\delta_{ij} r_{ij}} \sum_{k=0}^{10} \frac{(\delta_{ij} r_{ij})^k}{k!}$ and $f_2(r_{ij}) = 1 - e^{-\zeta_{ij} r_{ij}}$

Here the r_{ij} denote site-site distances, the q_i electric charges of sites, and the $C_{ij,n}$ dispersion coefficients; the leading dispersion term is always proportional to r_{ij}^{-6}. In both models the auxiliary N sites (compare Fig. 1), placed on the molecule axis halfways between the outer sites (H or O) and

the center (M), carry each a charge of $+q$, and the central M site a charge of $-2q$. The outer sites do not have electric charges. The two models differ mostly in the choice of the damping function $f_1(r_{ij})$: Eq. (4) makes use of the damping function of Tang and Toennies [34], which had also been built into many noble-gas pair potentials.

Fitting these functions to the *ab initio* interaction energy values proved difficult, because the object function of the fitting problem has got many local minima. For this work the global minima were coarsely located by means of a genetic algorithm, and then the parameters optimized with a Marquardt-Levenberg algorithm. The results - the parameters of the interaction potentials - are given in Tables 3 and 4.

4. Second virial coefficients

Virial coefficients are linked to intermolecular potentials by rigorous statistical thermodynamic theory; the second virial coefficient depends on the pair potential only. On the other hand, at least second virial coefficients have been determined experimentally for many gases. Hence the prediction of second virial coefficients from *ab initio* potentials is a stringent test for the usefulness of such potentials: Computer simulations of some property of the liquid state may fail to give satisfactory results because multi-body potentials could not be accounted for, or because that property is difficult to sample by simulations. But a failure to reproduce second virial coefficients points to an inadequacy of the pair potential used.

In the case of hydrogen the matter is more complicated because of quantum effects. These can in principle be obtained from a perturbation expansion of Planck's constant (for a more detailed explanation see [35]). The first order corrections to the second virial coefficient of linear molecules have been worked out by Pack [29] and Wang [36]. Following the latter, the virial coefficient up to first order can be written as

$$B(T)=\frac{N_\mathrm{A}}{2V\iint \mathrm{d}\Omega_1\mathrm{d}\Omega_2}\iiiint\left(1-\exp\left(\frac{-u}{k_\mathrm{B}T}\right)\left[1+\frac{1}{12(k_\mathrm{B}T)^2}H_0u\right]\right)\mathrm{d}\vec{r}_1\mathrm{d}\vec{r}_2\mathrm{d}\Omega_1\mathrm{d}\Omega_2 \tag{5}$$

Here N_A is Avogradro's constant, k_B Boltzmann's constant, T the temperature, and $u(r, \alpha, \beta, \varphi)$ the pair potential; its parameters, the center-center distance and the relative orientation angles must be calculate from the center vectors $\vec{r}_i$ and the absolute orientations Ω_i. H_0 is the translation-rotation Hamiltonian for a pair of molecules.

This expression can be broken down into a zeroth order (classical) term and first-order quantum corrections (radial part, angular part proportional to I^{-1} (moment of inertia), angular part proportional to μ^{-1} (reduced mass)):

$$B(T)=B^{(0)}(T)+B^1_\mathrm{r}(T)+B^1_{\mathrm{a},I}(T)+B^1_{\mathrm{a},\mu}(T) \tag{6}$$

The classical part is given by

$$B^{(0)}(T)=-\frac{N_\mathrm{A}}{4}\int_0^{2\pi}\int_0^{\pi}\sin\beta\int_0^{\pi}\sin\alpha\int_0^{\infty}\left(1-\exp\left(-\frac{u}{k_\mathrm{B}T}\right)\right)r^2\mathrm{d}r\mathrm{d}\alpha\mathrm{d}\beta\mathrm{d}\phi \tag{7}$$

The first-order correction terms can be written as:

$$B^1_r(T)=\frac{N_\mathrm{A}\hbar^2}{96\mu(k_\mathrm{B}T)^3}\int_0^{2\pi}\int_0^{\pi}\sin\beta\int_0^{\pi}\sin\alpha\int_0^{\infty}\exp\left(-\frac{u}{k_\mathrm{B}T}\right)\left(\frac{\partial u}{\partial r}\right)^2 r^2\mathrm{d}r\mathrm{d}\alpha\mathrm{d}\beta\mathrm{d}\phi \tag{8}$$

$$\begin{aligned}B^1_{\mathrm{a},I}(T)=-\frac{N_\mathrm{A}\hbar^2}{48(k_\mathrm{B}T)^2}\int_0^{2\pi}\int_0^{\pi}\sin\beta\int_0^{\pi}\sin\alpha\int_0^{\infty}\exp\left(-\frac{u}{k_\mathrm{B}T}\right)\sum_{l_1l_2l}u_{l_1l_2l}(r)A_{l_1l_2l}(\alpha,\beta,\phi)\\ \times\left(\frac{l_1(l_1+1)}{2I_1}+\frac{l_2(l_2+1)}{2I_2}\right)r^2\mathrm{d}r\mathrm{d}\alpha\mathrm{d}\beta\mathrm{d}\phi\end{aligned} \tag{9}$$

$$\begin{aligned}B^1_{\mathrm{a},\mu}=-\frac{N_\mathrm{A}\hbar^2}{48(k_\mathrm{B}T)^2}\int_0^{2\pi}\int_0^{\pi}\sin\beta\int_0^{\pi}\sin\alpha\int_0^{\infty}\exp\left(-\frac{u}{k_\mathrm{B}T}\right)\sum_{l_1l_2l}u_{l_1l_2l}(r)A_{l_1l_2l}(\alpha,\beta,\phi)\\ \times\frac{l(l+1)}{2\mu r^2}r^2\mathrm{d}r\mathrm{d}\alpha\mathrm{d}\beta\mathrm{d}\phi\end{aligned} \tag{10}$$

The terms $u_{l_1 l_2 l}(r)\mathrm{A}_{l_1\ l_2 l}(\alpha, \beta, \varphi)$ represent a spherical harmonics expansion of the interaction potential. All these integrals were evaluated numerically with a 4D Gauss–Legendre quadrature method [37]. The results for the second virial coefficients are presented in Tables 5 and 6.

5. Discussion

The predicted values for the second virial coefficents of hydrogen shown in Table 5 are in excellent agreement with the experimental data. It appears that values obtained with potential function (3) are marginally better than those obtained with potential function (4), although the latter function has more adjustable parameters. But the differences are insignificant.

More important is the fact that an accurate prediction of second virial coefficients from an *ab initio* pair potential without recourse to experimental data is possible, and that the CCSD(T) method, applied to basis sets aug-cc-pVDZ and aug-cc-pVTZ, and followed by an extrapolation to the basis set limit, is evidently able to generate virial coefficients almost within the uncertainties of the experiments (see Fig. 6).

It is worth noting that quantum corrections contribute significantly to the second virial coefficient of hydrogen even at high temperatures. Of these corrections, only the radial term is important; the angular terms are usually much smaller in size.

Experimental values for the cross virial coefficients of the hydrogen–oxygen interaction are difficult to find in the literature. There are some experiments, however, from which these virial coefficients can be calculated:

- Van Itterbeek and van Doninck measured the speed of sound in (hydrogen + oxygen) mixtures at low temperatures and pressures [38]. The pressure dependence of this property is related to the virial coefficients. The values of the cross virial coefficient obtained by these authors lie reasonably close to our predictions (see Table 6); it should be noted, however, that their evaluation method involved several simplifications (linearizations, neglect of temperature derivatives of the virial coefficient), and that their results exhibit an uncertainty of about 20%.
- McKinley at al. measured solid–fluid equilibria of the (hydrogen + oxygen) system [39]. With the usual assumptions and simplifications (no hydrogen dissolved in the solid oxygen, neglect of higher virial coefficients) it is possible to estimate cross second virial coefficients from these data. The result agrees reasonably well with the *ab initio* prediction. The sublimation pressure of γ-oxygen, which is required for the equilibrium calculation, was taken from the work of Roder [40].
- In an earlier publication on high-pressure phase equilibria of the (hydrogen + oxygen) system it had been suggested that the parameters of the hydrogen–oxygen interaction could be interpolated from those of the systems (hydrogen + nitrogen), (neon + nitrogen), and (neon + oxygen) [41]. This idea can be extended to second virial coefficients as follows: Eq. (7) can be simplified-although with some loss of accuracy-by performing the integrations of the orientation variables:

$$B^{(0)}(T) = -2\pi N_\mathrm{A} \int_0^\infty \left[\exp\left(-\frac{\bar{u}(r,T)}{k_\mathrm{B}T} \right) - 1 \right] r^2 \mathrm{d}r \tag{11}$$

Here $\bar{u}(r,T)$ denotes an angle-averaged pair potential. For small molecules like the ones studied here the assumption of conformal pair potentials is usually acceptable, i.e., pair potentials can be written as

$$\bar{u}(r,T) = \epsilon \tilde{u}(\tilde{r},\tilde{T}) \text{ with } \tilde{r} = \frac{r}{\sigma} \text{ and } \tilde{T} = \frac{k_\mathrm{B}T}{\epsilon} \tag{12}$$

where $\tilde{u}(\tilde{r},\tilde{T})$ is a universal (reduced) pair potential function. Then Eq. (11) become

$$B^{(0)}(T) = -2\pi N_\mathrm{A} \sigma^3 \int_0^\infty \left[\exp\left(-\frac{\bar{u}(\tilde{r},\tilde{T})}{\tilde{T}} \right) - 1 \right] \tilde{r}^2 \mathrm{d}\tilde{r} \tag{13}$$

We use this equation for the cross virial coefficient of the hydrogen–oxygen system, assuming $\epsilon_{\mathrm{H_2,O_2}} = \epsilon_{\mathrm{H_2,N_2}} + \Delta\epsilon_{\mathrm{O_2,N_2}}$, where the last term is supposed to be small. Taylor expansion of the Boltzmann factor of this term, truncation after the linear term, and rearrangement yield

$$\frac{B^{(0)}_{\mathrm{H_2,O_2}}(T)}{N_\mathrm{A}\sigma_{\mathrm{H_2,O_2}}} \approx \frac{B^{(0)}_{\mathrm{H_2,N_2}}(T)}{N_\mathrm{A}\sigma_{\mathrm{H_2,O_2}}} - 2\pi\frac{\Delta\epsilon_{\mathrm{O_2,N_2}}}{\tilde{T}_{\mathrm{H_2,N_2}}}\int_0^\infty \tilde{u}(\tilde{r},\tilde{T}_{\mathrm{H_2,N_2}})\left[\exp\left(-\frac{\tilde{u}(\tilde{r},\tilde{T}_{\mathrm{H_2,N_2}})}{\tilde{T}_{\mathrm{H_2,N_2}}}\right)-1\right]\tilde{r}^2\mathrm{d}\tilde{r} \qquad (14)$$

where the integral is a function of the reduced temperature $\tilde{T}$ only. A similar equation holds for the cross virial coefficients of the (neon + oxygen) and (neon + nitrogen) systems, for which experimental data are available [42]. Therefore $\Delta\epsilon_{\mathrm{O_2,N_2}}$ can be determined from the neon data and then substituted into Eq. (14) to give the second virial coefficient of (hydrogen + oxygen) at the same *reduced* temperature as the (neon + oxygen) system (tacitly assuming that this value also holds for the hydrogen systems). For the parameters ϵ and σ usual Lennard-Jones parameters [35] and Berthelot–Lorentz combining rules were used. It turns out that the hydrogen–oxygen cross virial coefficient obtained from this interpolation (−58 cm3/mol) agrees reasonably well with the *ab initio* predictions as well as with the experimental values (see Fig. 7).

Recently Estela-Uribe and Jaramillo [43] published empirical correlation equations for second virial coefficients which are based on the corresponding-states approach of Lee and Kesler [44]. In their work, binary interactions are characterized by so-called pseudocritical parameters, which are interpolations of the pure-fluid critical temperatures and densities:

$$\rho_{\mathrm{c},ij}^{-1/3} = \frac{1+d_{ij}}{2}(\rho_{\mathrm{c},i}^{-1/3}+\rho_{\mathrm{c},j}^{-1/3}) \text{ and } T_{\mathrm{c},ij} = \frac{(1-k_{ij})(T_{\mathrm{c},i}T_{\mathrm{c},j})^{1/2}}{1+c/(M_{ij}T)} \qquad (15)$$

$$\text{with } M_{ij}^{-1} = \frac{1}{2}(M_i^{-1}+M_j^{-1}) \text{ and } k_{ij} = 1-\frac{a_{ij}\rho_{\mathrm{c},ij}}{(\rho_{\mathrm{c},i}\rho_{\mathrm{c},j})^{1/2}}$$

Here the Mi denote molar masses of the pure components, M_{ij} an "interaction molar mass", and c is a constant (21.8 K g/mol) It turns out that the adjustable parameters a_{ij} and d_{ij} are very close to zero for a large number of chemical compounds.

We have set these two correlation parameters to zero for the hydrogen–oxygen interaction and used the correlations of Estela-Uribe and Jaramillo to predict cross second virial coefficents. The results, presented in Table 6, show a remarkably good agreement with the predictions from quantum mechanics.

We conclude that our *ab initio* pair potential for the hydrogen–oxygen interaction is reliable, and that the calculation of thermodynamic properties from quantum mechanical results can be useful, if experimental data are scarce.

6. Acknowledgments

The Regional Computer Center of Cologne (RRZK) contributed to this project by a generous allowance of computer time as well as by efficient software support; we especially wish to thank Dr. L. Packschies (RRZK) for technical help with the Gaussian03 software. We would like to thank Dr. P. K. Naicker and Dr. A. K. Sum (University of Delaware) for making available their computer program for virial coefficents.

References

1. S. D. Tse, D. L. Zhu, and C. K. Law, Morphology and burning rates of expanding spherical flames in H_2/O_2 inert mixtures up to 60 atmospheres, in *Proceedings of the Combustion Institute*, volume 28, pages 1793–1800. NASA (Glenn Research Center), 2000.
2. T. M. Haarmann and W. Koschel, Proc. Appl. Math. Mech., 2003, **2**, 360–361.
3. H. Popkie, H. Kistenmacher, and E. Clementi, J. Chem. Phys., 1973, **59**, 1325–1336.
4. U. K. Deiters, M. Hloucha, and K. Leonhard, Experiments? — No, thank you!, in T. M. Letcher, editor, *Chemistry for the 21st Century: Chemical Thermodynamics*, IUPAC Monograph Series, pages 187–195. Blackwell Science, Oxford, 1999.
5. R. Eggenberger, S. Gerber, H. Huber, and M. Welcker, Mol. Phys., 1994, **82**, 689–699.
6. E. Ermakova, J. Solca, H. Huber, and D. Marx, Chem. Phys. Lett., 1995, **246**, 204–208.
7. E. Ermakova, J. Solca, G. Steinebrunner, and H. Huber, Chem. Eur. J., 1998, **4**, 377–382.
8. B. Kirchner, E. Ermakova, J. Solca, and H. Huber, Chem. Eur. J., 1998, **4**, 383–388.
9. M. Venkatraj, C. Bratschi, H. Huber, and R. J. Gdanitz, Fluid Phase Equilib., 2004, **218**, 285–289.
10. S. L. Garrison and S. I. Sandler, J. Chem. Phys., 2002, **117**, 10571–10580.

11. A. Malijevsk´y and A. Malijevsk´y, Mol. Phys., 2003, **101**, 3335–3340.
12. T. Korona, H. L. Williams, R. Bukowski, B. Jeziorski, and K. Szalewicz, J. Chem. Phys., 1997, **106**, 5109–5122.
13. A. E. Nasrabad and U. K. Deiters, J. Chem. Phys., 2003, **119**, 947–952.
14. A. E. Nasrabad, R. Laghaei, and U. K. Deiters, J. Chem. Phys., 2004, **121**, 6423–6434.
15. A. E. Nasrabad and R. Laghaei, Computational Studies on Thermodynamic Properties, Effective Diameters, And Free Volume of Argon Using an *ab initio* Potential, J. Chem. Phys 2006; **125**, 084510.
16. J. López Cacheiro, B. Fernandez, D. Marchesan, S. Coriani, C. Hattig, and A. Rizzo, J. Mol. Phys., 2004, **102**, 101–110.
17. K. Leonhard and U. K. Deiters, Mol. Phys., 2002, **100**, 2571–2585.
18. S. Bock, E. Bich, and E. Vogel, Chem. Phys., 2000, **257**, 147–156.
19. R. T. Pack, J. Chem. Phys., 1983, **78**, 7217–7222.
20. P. K. Naicker, A. K. Sum, and S. I. Sandler, J. Chem. Phys., 2003, **118**, 4086–4093.
21. A. Z. Panagiotopoulos, J. Phys. Condensed Matter, 2000, **12**, R25–52.
22. P. Diep and J. K. Johnson, J. Chem. Phys., 2000, **112**, 4465–4473.
23. P. Diep and J. K. Johnson, J. Chem. Phys, 2000, **113**, 3480–3481.
24. L. E. Sutton, editor, *Table of Interatomic Distances and Configurations in Molecules and Ions: supplement 1956–1959*. Number 18 in Special publication. Chemical Society, London, 1965.
25. R. A. Kendall, T. H. Dunning, Jr., and R. J. Harrison, J. Chem. Phys., 1992, **96**, 6796–6806.
26. S. F. Boys and F. Bernardi, Mol. Phys., 1970, **19**, 553–566.
27. P. L. Fast, M. L. Sanchez, and D. G. Truhlar, J. Chem. Phys., 1999, **111**, 2921–2926.
28. W. Klopper, in J. Grotendorst, editor, *Modern Methods and Algorithms of Quantum Chemistry*, NIC series, page 153. John von Neumann Institute, J¨ulich, 2000.
29. W. Klopper, Mol. Phys., 2001, **99**, 481–507.
30. S. Y. Park and L. J. Sh., J. Chem. Phys., 2002, **116**, 5389–5394.
31. K. Leonhard and U. K. Deiters, Mol. Phys., 2000, **98**, 1603–1616.
32. Gaussian03, Revision B.02. Gaussian Inc., Wallingford, CT, USA, 2003.
33. V. Aquilanti, M. Bartolomei, D. Cappelletti, E. Carmona-Novillo, and F. Pirani, J. Chem. Phys., 2002, **117**, 615–627.
34. K. T. Tang and J. P. Toennies, J. Chem. Phys., 1984, **80**, 3726–3741.
35. J. O. Hirschfelder, C. F. Curtiss, and R. B. Bird, *Molecular Theory of Gases and Liquids*. John Wiley, New York, 1954.
36. W. F. Wang, J. Quant. Spectrosc. Radiat. Transfer, 2003, **76**, 23–30.
37. W. Squire, *Integration for Engineers and Scientists*. Elsevier, New York, 1970.
38. A. van Itterbeek and W. van Doninck, Proc. Phys. Soc. London B, 1949, **62**, 62–69.
39. C. McKinley, J. Brewer, and W. E. S. J., Adv. Cryogen. Eng., 1961, **7**, 114–124.
40. H. M. Roder, *The Thermodynamic Properties of Slush Hydrogen and Oxygen*. NBSIR 77-859. National Bureau of Standards, Boulder, 1977.
41. U. K. Deiters, M. Neichel, and E. U. Franck, Ber. Bunsenges. Phys. Chem., 1993, **97**, 649–657.
42. J. H. Dymond and E. B. Smith, *The Virial Coefficients of Pure Gases and Mixtures*. Clarendon Press, Oxford, 1980.
43. J. F. Estela-Uribe and J. Jaramillo, Fluid Phase Equilib., 2005, **231**, 84–98.
44. B. I. Lee and M. G. Kesler, AIChE J., 1975, **21**, 510–527.
45. D. R. Lide, editor, *Handbook of Chemistry and Physics*. CRC Press, Boca Raton, 85th edition, 2000.
46. R. D. Etters, R. Danilowicz, and W. England, Phys. Reviews A, 1975, **12**, 2199–2212.
47. N. B. Vargaftik, *Tables on the Thermophysical Properties of Liquids and Gases in Normal and Dissociated States*. Wiley, New York, 1975.

Table 1: Potential energies E_{min} and equilibrium distances r_{min} of dimers at selected orientations (α, β, ϕ), calculated with CCSD(T) method and basis sets aug-cc-pVmZ with m = 2, 3, 23.

			aug-cc-pVDZ		aug-cc-pVTZ		aug-cc-pV23Z	
α	β	ϕ	r_{min}/Å	$10^6 E_{min}/E_H$	r_{min}/Å	$10^6 E_{min}/E_H$	r_{min}/Å	$10^6 E_{min}/E_H$
				H_2-H_2				
0	0	0	3.8	-42.3549	3.8	-37.4896	3.8	-35.444
90	0	0	3.6	-110.267	3.4	-152.745	3.4	-171.825
90	90	0	3.8	-32.6377	3.6	-47.3085	3.6	-55.246
90	90	90	3.8	-42.7146	3.6	-66.9307	3.4	-78.1582
				H_2-O_2				
0	0	0	4.0	-176.903	4.0	-225.514	3.8	-247.957
90	0	0	4.0	-167.764	3.8	-237.364	3.8	-268.209
90	90	0	3.4	-200.841	3.2	-332.693	3.0	-398.079
90	90	90	3.6	-84.2173	3.4	-156.328	3.2	-196.486

Table 2: Comparison of bond lengths of the hydrogen–oxygen dimer in an optimized T configuration (α = 90, β = ϕ = 0), calculated with the CCSD(T) method and different basis sets.

Basis set	$r_{H\text{-}H}$/Å	$r_{O\text{-}O}$/Å
aug-cc-pVDZ	0.761677	1.233374
aug-cc-pVTZ	0.742979	1.223396
aug-cc-pV23Z	0.735106	1.219195
Exp [46]	0.7413	1.207411

Table 3: Optimized parameters of the 5-site potential function (3). Partial charges: hydrogen: q_N/e = –0.078329, q_H = 0; oxygen: q_N/e = –0.98630, q_O = 0; q_M = -2q_N. E_H = 4.359782×10^{-18} J (Hartree energy unit).

interaction	De/E_H	α/Å^{-1}	(C_6/E_H)/Å^6	(C_6/E_H)/Å^8	(C_6/E_H)/Å^{10}
			H_2-H_2		
H-H	1.0228×10^{-1}	0.5726	1.3331×10^1	-6.0553×10^1	1.1427×10^2
H-N	-7.6904×10^{-1}	2.8339	-4.8925×10^1	2.2518×10^2	-4.1995×10^2
H-M	-1.9219×10^{-1}	0.5715	7.0556×10^1	-3.2310×10^2	6.0229×10^2
M-M	-4.9352×10^{-2}	0.5773	-2.9216×10^2	1.3811×10^3	-2.5920×10^3
M-N	4.1656×10^0	3.0343	1.9574×10^2	-9.2093×10^2	1.7195×10^3
N-N	5.5669×10^{-1}	0.5726	4.4158×10^2	-2.1135×10^3	3.9999×10^3
			H_2-O_2		
H-O	6.9772×10^1	2.2167	4.3122×10^1	-1.7085×10^2	1.9864×10^2
H-N	-8.6380×10^2	2.8495	-2.8926×10^2	1.7056×10^3	-2.0407×10^3
H-M	5.9249×10^3	3.2500	7.0326×10^2	-6.6618×10^3	8.8238×10^3
N-O	-1.1945×10^2	2.2241	-2.0153×10^2	8.1092×10^2	-1.6856×10^3
N-N	5.2939×10^2	2.4593	-2.9395×10^2	2.8724×10^3	-4.8864×10^3
N-M	-3.4254×10^3	3.4888	5.4258×10^2	-5.1390×10^3	9.0644×10^3
M-O	3.4040×10^2	3.1597	4.6619×10^2	-1.9659×10^3	4.0898×10^3
M-M	-1.3311×10^3	2.4629	-1.5500×10^3	1.7298×10^4	-2.7469×10^4

Table 4: Optimized parameters of the 5-site potential function (4). For all interactions $\delta_{ij} = 5.0$ Å^{-1} and $\zeta_{ij} = 1.0$Å^{-1} were assumed. See Table 3 for the partial charges.

interaction	De/E_H	α/Å^{-1}	(C_6/E_H)/Å^6	(C_6/E_H)/Å^8	(C_6/E_H)/Å^{10}	(C_6/E_H)/Å^{12}
			H_2-H_2			
H-H	-6.784×10^{0}	1.9231	4.262×10^{1}	-3.153×10^{1}	2.163×10^{2}	-1.655×10^{2}
H-N	-5.820×10^{1}	2.3929	-7.308×10^{1}	2.987×10^{2}	-3.550×10^{2}	6.276×10^{2}
H-M	8.196×10^{1}	2.1509	3.680×10^{1}	-2.863×10^{2}	-1.458×10^{2}	-2.134×10^{2}
M-M	-9.521×10^{1}	2.1064	-8.199×10^{2}	4.323×10^{3}	-1.609×10^{4}	2.516×10^{4}
M-N	1.110×10^{2}	2.3557	5.208×10^{2}	-2.478×10^{3}	8.087×10^{3}	-1.198×10^{4}
N-N	8.194×10^{1}	1.9595	1.464×10^{3}	-8.550×10^{3}	3.523×10^{4}	-5.773×10^{4}
			H_2-O_2			
H-O	8.031×10^{2}	2.5442	-2.413×10^{2}	-6.748×10^{2}	-5.092×10^{3}	2.801×10^{3}
H-N	-2.443×10^{4}	3.9714	6.479×10^{2}	-1.035×10^{4}	5.657×10^{4}	-3.314×10^{4}
H-M	9.773×10^{4}	3.8896	-1.060×10^{3}	2.357×10^{4}	-1.968×10^{5}	9.897×10^{4}
N-O	-3.738×10^{3}	2.6003	5.700×10^{2}	7.742×10^{3}	6.132×10^{3}	7.740×10^{3}
N-N	2.776×10^{3}	2.8975	-6.953×10^{2}	-7.366×10^{2}	6.722×10^{3}	-3.054×10^{4}
N-M	-2.535×10^{4}	3.7516	8.308×10^{2}	7.766×10^{2}	-7.083×10^{3}	8.570×10^{4}
M-O	4.950×10^{3}	2.5963	-7.921×10^{2}	-1.099×10^{4}	-4.793×10^{3}	-1.450×10^{4}
M-M	-5.654×10^{3}	2.8208	-7.416×10^{2}	-1.262×10^{4}	1.848×10^{5}	-3.081×10^{5}

Table 5: Second virial coefficients of hydrogen as a function of temperature (given in cm^3/mol). B0: classical result obtained from pair potential, $B_r^{(1)}$, $B_{a,I}^{(1)}$, $B_{a,\mu}^{(1)}$: quantum corrections, B: total virial coefficient; methods: Eq. (3) and Eq. (4): predicted *ab initio* using these two pair potentials, exp.: experimental data.

T/K	method	$B^{(0)}$	$B_r^{(1)}$	$B_{a,I}^{(1)}$	$B_{a,\mu}^{(1)}$	B	ref.
60	Eq.(3)	-24.655	0.626	0.049	0.01	-23.970	
	Eq.(4)	-24.408	0.356	0.076	0.026	-26.321	
	exp.					-24.000	[45]
70	Eq.(3)	-16.307	0.288	0.044	0.005	-15.970	
	Eq.(4)	-16.144	0.117	0.066	0.012	-17.178	
	exp.					-16.000	[45]
75	Eq.(3)	-13.107	1.065	0.055	0.017	-11.970	
	Eq.(4)	-12.976	0.9	0.099	0.027	-10.799	
	exp.					-12.000	[42]
80	Eq.(3)	-10.373	1.382	0.059	0.022	-8.910	
	Eq.(4)	-10.269	1.233	0.113	0.033	-8.782	
	exp.					-8.940	[46]
90	Eq.(3)	-5.96	0.884	0.052	0.014	-5.010	
	Eq.(4)	-5.900	0.791	0.094	0.025	-6.140	
	exp.					-5.040	[46]
100	Eq.(3)	-3.066	0.034	0.041	0.001	-2.990	
	Eq.(4)	-3.036	0.014	0.061	0.01	-0.982	
	exp.					-3.000	[45]
109.01	Eq.(3)	-0.127	0.511	0.047	0.008	0.440	
	Eq.(4)	-0.125	0.485	0.081	0.019	-0.117	

T/K	method	$B^{(0)}$	$B_r^{(1)}$	$B_{a,I}^{(1)}$	$B_{a,\mu}^{(1)}$	B	ref.
	exp.					0.410	[42]
123.15	Eq.(3)	2.867	0.071	0.041	0.001	2.980	
	Eq.(4)	2.838	0.086	0.064	0.011	2.906	
	exp.					2.950	[42]
133.27	Eq.(3)	4.553	0.561	0.048	0.009	5.170	
	Eq.(4)	4.507	0.577	0.085	0.021	4.589	
	exp.					5.140	[42]
150	Eq.(3)	6.751	0.329	0.045	0.005	7.130	
	Eq.(4)	6.684	0.373	0.077	0.017	6.763	
	exp.					7.100	[42]
173.15	Eq.(3)	8.962	0.029	0.04	0.0000	9.030	
	Eq.(4)	8.872	0.036	0.062	0.01	8.934	
	exp.					8.930	[42]
223.15	Eq.(3)	11.859	0.176	0.043	0.003	12.080	
	Eq.(4)	11.74	0.273	0.072	0.015	11.793	
	exp.					12.050	[42]
265.6	Eq.(3)	13.246	1.111	0.055	0.018	14.430	
	Eq.(4)	13.113	1.193	0.111	0.032	13.212	
	exp.					14.400	[47]
298.8	Eq.(3)	13.957	1.051	0.055	0.017	15.080	
	Eq.(4)	13.818	1.142	0.109	0.031	13.983	
	exp.					15.050	[47]
398.15	Eq.(3)	15.073	0.755	0.05	0.012	15.890	
	Eq.(4)	14.922	0.864	0.098	0.026	15.377	
	exp.					15.860	[42]

Table 6: Cross second virial coefficients of the hydrogen–oxygen system. correl.: empirical correlation [42], exp.: experimental data. For an explanation of the other properties see Table 5.

T/K	method	$B^{(0)}$	$B_r^{(1)}$	$B_{a,I}^{(1)}$	$B_{a,\mu}^{(1)}$	B	ref.
49.8	Eq. (3)	−138.393	0.199	0.266	0.053	−137.876	
	Eq. (4)	−137.023	0.057	0.037	0.028	−136.900	
	correl.					−142.097	
	exp.					−110.0	[39]
60.00	Eq. (3)	−100.725	0.104	0.209	0.042	−100.370	
	Eq. (4)	−99.728	0.020	0.010	0.019	−99.679	
	correl.					−106.393	
80.00	Eq. (3)	−60.795	0.228	0.283	0.057	−60.227	
	Eq. (4)	−59.559	0.036	0.096	0.032	−60.154	
	correl.					−63.887	
	exp.					−72.9	[38]
85.00	Eq. (3)	−57.374	0.405	0.388	0.078	−56.504	
	Eq. (4)	−56.806	0.325	0.073	0.057	−56.352	
	correl.					−56.806	
	exp.					−54.0	[38]
90.00	Eq. (3)	−49.970	0.344	0.352	0.070	−49.204	

T/K	method	$B^{(0)}$	$B_r^{(1)}$	$B_{a,I}^{(1)}$	$B_{a,\mu}^{(1)}$	B	ref.
	Eq. (4)	−48.627	0.192	0.042	0.046	−49.113	
	correl.					−50.664	
	exp.					−32.5	[38]
100.00	Eq. (3)	−41.612	0.427	0.401	0.080	−40.705	
	Eq. (4)	−40.200	0.299	0.066	0.055	−40.602	
	correl.					−40.591	
123.15	Eq. (3)	−27.115	0.490	0.438	0.088	−26.099	
	Eq. (4)	−25.729	0.387	0.085	0.063	−25.987	
	correl.					−24.782	
150.00	Eq. (3)	−15.285	0.449	0.414	0.083	−14.340	
	Eq. (4)	−14.093	0.344	0.076	0.059	−14.234	
	correl.					−13.804	
200.00	Eq. (3)	−3.798	0.426	0.400	0.080	−2.891	
	Eq. (4)	−2.761	0.323	0.071	0.057	−2.789	
	correl.					−2.789	
273.15	Eq. (3)	4.077	0.406	0.388	0.078	4.948	
	Eq. (4)	4.998	0.302	0.067	0.055	5.048	
	correl.					4.656	
298.15	Eq. (3)	5.101	0.429	0.402	0.080	6.012	
	Eq. (4)	5.545	0.365	0.080	0.061	5.600	
	correl.					6.165	
400.00	Eq. (3)	8.636	0.448	0.260	0.082	9.425	
	Eq. (4)	9.623	0.345	0.076	0.059	9.720	
	correl.					9.931	

Table 7: Pair interaction energies calculated with the CCSD(T) method and the basis sets aug-cc-pVmZ, m = 2, 3, 23*.

				$10^6u/E_H$ H_2–H_2				$10^6u/E_H$ H_2–O_2		
α	β	ϕ	r/Å	m = 2	m = 3	m = 23	r/Å	m = 2	m = 3	m = 23
0	0	0	2.8	978.17	877.59	835.3	3.4	473.71	291.25	214.42
0	0	0	3	398.31	342.95	319.67	3.6	17.12	-98	-146.47
0	0	0	3.4	11.64	2.86	-0.83	3.8	-142.28	-216.65	-247.96
0	0	0	3.6	-31.77	-31.2	-30.96	4	-176.9	-225.51	-245.98
0	0	0	3.8	-42.35	-37.49	-35.44	4.2	-164.03	-196.57	-210.27
0	0	0	5	-10.94	-7.15	-12.23	5	-67.83	-76.03	-79.48
0	0	0	10	0.1	0.22	-5.55	10	-0.98	-1.1	-1.15
45	0	0	3	238.21	144.38	104.93	3.4	287.21	115.78	43.59
45	0	0	3.2	31.66	-22.89	-45.82	3.6	-50.97	-162.59	-209.59
45	0	0	3.4	-49.09	-79.91	-92.87	3.8	-160.79	-233.45	-264.04
45	0	0	3.6	-71.87	-89	-96.2	4	-176.12	-223.52	-243.48
45	0	0	4	-60.52	-65.57	-52.8	4.2	-157.1	-188.29	-201.43
45	0	0	5	-18.13	-18.14	-23.67	5	-62.67	-69.64	-72.58
45	0	0	10	-0.19	-0.16	-5.29	10	-0.62	-0.67	-0.69
90	0	0	2.8	449.78	265.06	187.4	3.2	807.44	556.85	451.34
90	0	0	3	87.81	-27.16	-75.5	3.4	159.81	-11.82	-84.08
90	0	0	3.2	-60.56	-131.85	-152.87	3.6	-89.41	-203.25	-251.18
90	0	0	3.4	-107.37	-152.75	-100.72	3.8	-164.11	-237.36	-268.21

				$10^6u/E_H$ H_2–H_2				$10^6u/E_H$ H_2–O_2		
α	β	ϕ	r/Å	m = 2	m = 3	m = 23	r/Å	m = 2	m = 3	m = 23
90	0	0	3.6	-110.27	-140.26	-79.08	4	-167.76	-213.85	-233.25
90	0	0	3.8	-97.07	-117.62	-61.77	4.2	-146.14	-174.93	-187.05
90	0	0	5	-24.89	-28.44	-10.31	5	-57.05	-62.49	-64.78
90	0	0	10	-0.47	-0.54	-0.57	10	-0.7	-0.25	-0.05
135	45	0	2.8	492.22	292.59	208.66	3.2	703.34	491.6	402.45
135	45	0	3	118.26	-5.71	-57.84	3.4	165.69	21.23	-39.59
135	45	0	3.2	-38.94	-115.77	-145.14	3.6	-59.89	-156.4	-197.04
135	45	0	3.4	-92.51	-141.03	-120.49	3.8	-138.56	-201.86	-228.51
135	45	0	3.6	-100.34	-131.88	-96.3	4	-151.61	-192.6	-209.85
135	45	0	3.8	-90.5	-111.61	-75.57	4.2	-138.06	-164.98	-176.32
135	45	0	4	-23.87	-27.03	-28.36	5	-61.12	-66.61	-68.93
135	45	0	9	-0.43	-0.49	-0.51	10	-1.07	-1.1	-1.11
90	45	0	2.8	160.83	59.21	16.48	3.4	401.94	235.32	165.16
90	45	0	3	4.84	-56.2	-81.87	3.6	125.17	19.35	-25.21
90	45	0	3.2	-52.98	-90.72	-106.59	3.8	4.99	-61.15	-89
90	45	0	3.4	-66.99	-91.14	-101.29	4	-40.54	-81.96	-99.4
90	45	0	3.6	-63.37	-79.31	-86.02	4.2	-52.23	-78.68	-89.81
90	45	0	3.8	-54	-64.82	-69.37	5	-28.77	-34.09	-36.33
90	45	0	5	-0.49	-0.53	-0.55	9	-0.66	-0.71	-0.73
90	45	0	9	-0.26	-0.28	-0.29	10	-0.33	-0.33	-0.33
45	45	0	2.8	739.82	595.17	534.36	3.2	810.42	586.92	492.81
45	45	0	3	288.53	205.82	171.04	3.4	223.04	72.17	8.65
45	45	0	3.2	81.12	36.46	17.69	3.6	-22.84	-125.08	-168.12
45	45	0	3.4	-5.82	-28.77	-38.42	3.8	-110.71	-179.48	-208.43
45	45	0	3.6	-36.22	-47.39	-52.09	4	-128.82	-175.01	-194.46
45	45	0	3.8	-41.97	-46.92	-49.01	4.2	-118.98	-149.99	-163.05
45	45	0	4	-38.2	-39.93	-40.66	5	-50.57	-57.96	-61.07
45	45	0	10	-0.02	0.04	0.07	10	-0.63	-0.72	-0.76
90	90	0	3	214.91	132.94	98.47	2.6	1027.94	576.3	386.14
90	90	0	3.2	58.37	9.44	-11.14	2.8	229.37	-91.39	-226.45
90	90	0	3.4	-6.08	-36.17	-48.83	3	-90.33	-306.9	-398.08
90	90	0	3.6	-28.43	-47.31	-55.25	3.2	-192.28	-332.69	-391.81
90	90	0	3.8	-32.64	-44.62	-49.66	3.4	-200.84	-290.2	-327.82
90	90	0	4	-29.91	-37.48	-40.66	3.8	-140.24	-177.7	-193.47
90	90	0	5	-9.46	-10.23	-10.56	5	-27.11	-31.82	-33.8
90	90	0	10	-0.06	-0.03	-0.02	10	-0.14	-0.19	-0.21
90	45	45	2.8	506.51	330.85	256.99	3.2	947.1	727.25	634.67
90	45	45	3.2	-2.17	-66.13	-93.02	3.4	426.61	244.04	167.17
90	45	45	3.4	-57.96	-97.96	-114.78	3.6	145.35	22.64	-29.03
90	45	45	3.6	-70.65	-96.55	-107.43	3.8	21.45	-61.22	-96.03
90	45	45	3.8	-66.14	-83.43	-90.7	4	-26.61	-83.38	-107.28
90	45	45	4	-56.14	-68	-72.98	4.4	-44.83	-66.7	-75.9
90	45	45	5	-17.74	-20.14	-21.15	5	-26	-30.6	-32.54
90	45	45	10	-0.29	-0.32	-0.33	10	-0.31	-0.65	-0.8
45	45	45	3	258.05	166.13	127.49	3.2	680.09	464.3	373.43
45	45	45	3.2	59.68	8.16	-13.5	3.4	174.49	28.34	-33.2

				$10^6u/E_H$ H_2–H_2				$10^6u/E_H$ H_2–O_2		
α	β	ϕ	r/Å	m = 2	m = 3	m = 23	r/Å	m = 2	m = 3	m = 23
45	45	45	3.4	-21.31	-49.49	-61.34	3.6	-43.3	-160.77	-210.23
45	45	45	3.6	-47.68	-62.9	-69.29	3.8	-119.69	-205.85	-242.13
45	45	45	3.8	-50.64	-58.74	-62.15	4	-132.43	-196.64	-223.68
45	45	45	4	-44.89	-49.08	-50.84	4.2	-119.75	-169.44	-190.37
45	45	45	5	-13.57	-13.3	-13.18	5	-53.29	-66.35	-71.84
45	45	45	10	-0.09	-0.05	-0.03	10	-0.27	-1.3	-1.73
90	90	45	2.8	534.9	387.27	325.2	2.8	445.33	123.89	-11.46
90	90	45	3.2	45.22	-8.38	-30.91	3	49.63	-164.9	-255.23
90	90	45	3.4	-15.32	-49.32	-63.62	3.2	-98.9	-236.46	-294.37
90	90	45	3.6	-35.15	-57.18	-66.44	3.4	-136.78	-223.35	-259.81
90	90	45	3.8	-37.67	-52.14	-58.23	3.6	-129.43	-184.36	-207.49
90	90	45	4	-33.69	-43.29	-47.33	4	-84.07	-107.88	-117.9
90	90	45	5	-10.82	-12.16	-12.73	5	-20.44	-24.7	-26.49
90	90	45	10	-0.11	-0.1	-0.09	10	0.01	-0.02	-0.04
90	45	90	2.8	491.26	310.36	234.3	3.4	444.91	281.94	213.31
90	45	90	3.2	-9.18	-76.07	-104.2	3.6	158.97	56.32	13.09
90	45	90	3.4	-62.94	-105.21	-122.98	3.8	31.49	-31.62	-58.2
90	45	90	3.6	-74.31	-101.95	-113.57	4	-19.3	-58.2	-74.58
90	45	90	4	-58.29	-71.17	-76.58	4.4	-36.08	-51.65	-58.2
90	45	90	5	-18.48	-21.17	-22.3	5	-20.7	-25.18	-27.07
90	45	90	10	-0.31	-0.35	-0.37	10	-0.03	0	0.01
45	45	90	2.8	598.82	418.3	342.4	3.2	558.82	353.11	266.49
45	45	90	3.2	13.24	-51.63	-78.9	3.4	120.11	-37.47	-103.82
45	45	90	3.4	-54.81	-93.45	-109.7	3.6	-71.12	-185.13	-233.13
45	45	90	3.6	-72.45	-95.9	-105.75	3.8	-136.31	-219.43	-254.43
45	45	90	3.8	-69.39	-83.95	-90.07	4	-143.45	-205.58	-231.74
45	45	90	4	-59.36	-68.63	-72.53	4.2	-127.99	-174.87	-194.61
45	45	90	5	-18.4	-19.77	-20.35	5	-56.16	-66.44	-70.77
45	45	90	10	-0.25	-0.26	-0.26	10	-0.54	-0.73	-0.81
90	90	90	2.8	507.94	353.01	287.87	2.8	661.35	339.17	203.51
90	90	90	3.2	32.44	-25.85	-50.35	3	189.43	-22.78	-112.13
90	90	90	3.4	-24.45	-62.26	-78.16	3.2	-5.97	-140.04	-196.49
90	90	90	3.6	-41.85	-66.93	-77.48	3.4	-72.74	-156.33	-191.52
90	90	90	3.8	-42.71	-59.6	-66.7	3.6	-84.22	-136.7	-158.8
90	90	90	5	-12.18	-14.09	-14.89	4	-60.13	-82.43	-91.82
90	90	90	9	-0.31	-0.33	-0.33	5	-13.79	-17.56	-19.15
90	90	90	10	-0.16	-0.16	-0.17	10	0.16	0.15	0.14
45	135	45	2.8	519.9	324.36	242.14	3.2	630.41	423.82	336.84
45	135	45	3	137.53	16.77	-34	3.4	142.78	-15.45	-82.07
45	135	45	3.2	-25.28	-99.4	-130.56	3.6	-66.19	-179.49	-227.19
45	135	45	3.4	-82.64	-128.83	-148.25	3.8	-138.13	-220.15	-254.68
45	135	45	3.6	-93.04	-122.62	-135.05	4	-148.27	-208.14	-233.34
45	135	45	3.8	-84.97	-104.47	-112.67	4.2	-133.3	-178.43	-197.43
45	135	45	5	-22.43	-25.14	-26.27	5	-60.49	-68.31	-71.61
45	135	45	9	-0.7	-0.78	-0.82	10	-0.99	-0.02	0.39

*:“23” denotes the extrapolation from sets 2 and 3

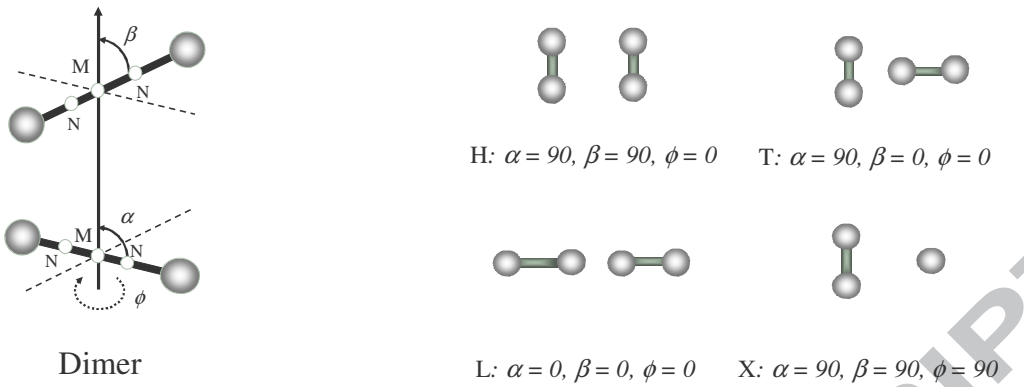

Fig. 1: 5-site molecular model and some selected orientations used for quantum chemical calculations.

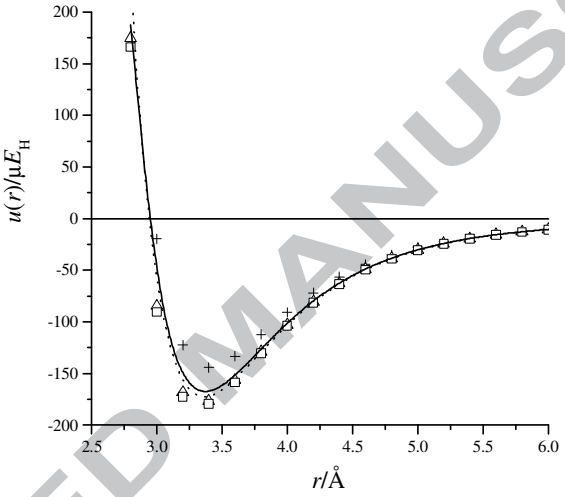

Fig. 2: Intermolecular potential of the hydrogen dimer in T configuration calculated with the basis set aug-cc-pVTZ with different post-SCF techniques: +: MP2, Δ: MP3, □: MP4, —: CCSD(T).

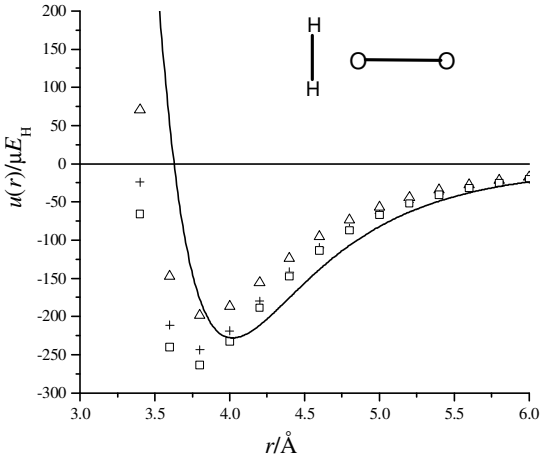

Fig. 3: Intermolecular potential of the hydrogen–oxygen dimer in T configuration calculated with the basis set aug-cc-pVTZ with different post-SCF techniques; for an explanation of the symbols see Fig. 2.

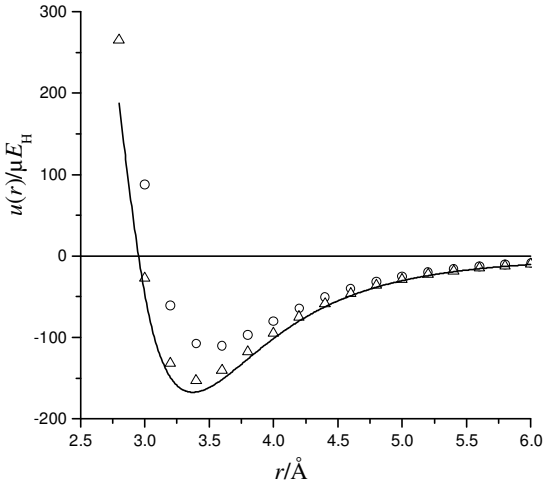

Fig. 4: Intermolecular potential of the hydrogen dimer in T configuration calculated with the CCSD(T) method for different basis sets: ○: aug-cc-pVDZ, Δ: aug-cc-pVTZ, —: aug-cc-pV23Z.

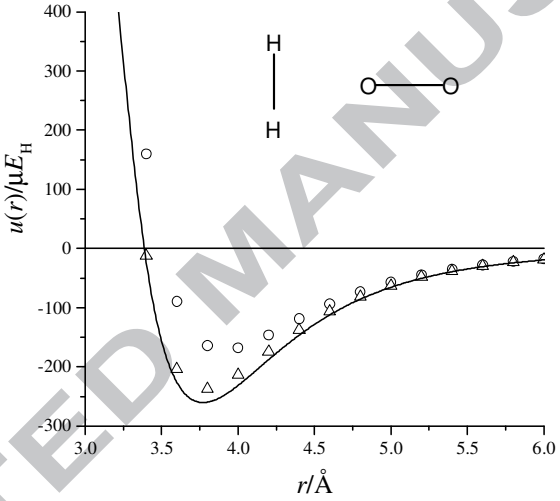

Fig. 5: Intermolecular potential of the hydrogen–oxygen dimer in T configuration calculated with the CCSD(T) method for different basis sets; for an explanation of the symbols see Fig. 4.

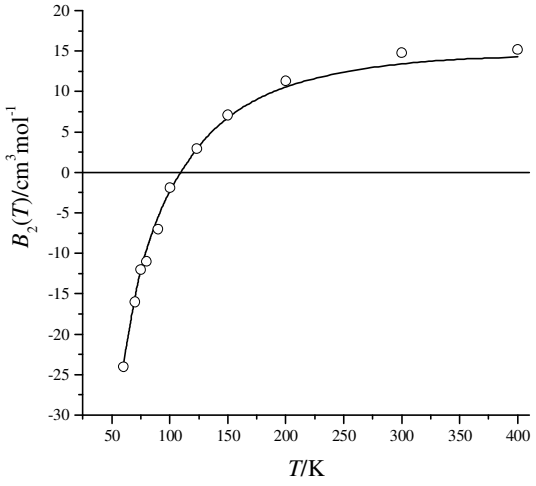

Fig. 6: Second virial coefficient of hydrogen. —: *ab initio* prediction (this work), symbols: experimental data (see Table 5).

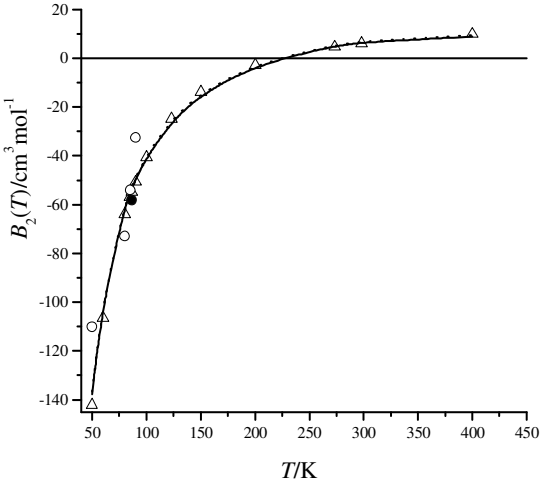

Fig. 7: Cross second virial coefficient of the hydrogen–oxygen system. —: *ab initio* prediction (this work) based on Eq. (3), - - -: prediction based on Eq. (4), 4: empirical correlation [43], •: interpolation from neon mixtures (see text), other symbols: experimental data (see Table 6).

Highlights

- We construct the angular orientations of dimers H_2-H_2 and H_2-O_2
- We calculate the *ab initio* intermolecular interaction energies for all built orientations.
- Extrapolating the interaction energies to the complete basis set limit aug-cc-pV23Z.
- We develop two 5-site *ab initio* intermolecular potentials of dimers H_2-H_2, H_2-O_2.
- Calculating the virial coefficients of dimer H_2-H_2 and H_2-O_2

Graphical abstract